

# Introducing process analytical technology (PAT) in filamentous cultivation process development: comparison of advanced online sensors for biomass measurement

Nanna Petersen Rønneest · Stuart M. Stocks ·  
Anna Eliasson Lantz · Krist V. Gernaey

Received: 15 October 2010 / Accepted: 9 March 2011 / Published online: 2 April 2011  
© Society for Industrial Microbiology 2011

**Abstract** The recent process analytical technology (PAT) initiative has put an increased focus on online sensors to generate process-relevant information in real time. Specifically for fermentation, however, introduction of online sensors is often far from straightforward, and online measurement of biomass is one of the best examples. The purpose of this study was therefore to compare the performance of various online biomass sensors, and secondly to demonstrate their use in early development of a filamentous cultivation process. Eight *Streptomyces coelicolor* fed-batch cultivations were run as part of process development in which the pH, the feeding strategy, and the medium composition were varied. The cultivations were monitored in situ using multi-wavelength fluorescence (MWF) spectroscopy, scanning dielectric (DE) spectroscopy, and turbidity measurements. In addition, we logged all of the classical cultivation data, such as the carbon dioxide evolution rate (CER) and the concentration of dissolved oxygen. Prediction models for the biomass concentrations were estimated on the basis of

the individual sensors and on combinations of the sensors. The results showed that the more advanced sensors based on MWF and scanning DE spectroscopy did not offer any advantages over the simpler sensors based on dual frequency DE spectroscopy, turbidity, and CER measurements for prediction of biomass concentration. By combining CER, DE spectroscopy, and turbidity measurements, the prediction error was reduced to 1.5 g/l, corresponding to 6% of the covered biomass range. Moreover, by using multiple sensors it was possible to check the quality of the individual predictions and switch between the sensors in real time.

**Keywords** Real-time monitoring · Biomass · Filamentous fermentation · Dielectric spectroscopy · Multi-wavelength fluorescence spectroscopy · Software sensors

## Introduction

Real-time measurement of biomass concentration could be very useful for many cultivation processes. However, despite the development of a number of promising technologies, accurate measurement of biomass concentration in real time remains a significant challenge—particularly for highly aerated and agitated cultivations of organisms with complex morphology. The challenges of biomass measurement have been excellently reviewed by Kiviharju et al. [17], Madrid and Felice [20], and Olsson and Nielsen [27]. The online sensors typically applied for biomass concentration measurement include sensors based on dielectric spectroscopy (DE), software sensors based on classical process monitoring data, and optical sensors of several kinds: online turbidity probes, near-infrared (NIR) reflectance and transmission probes, and multi-wavelength fluorescence (MWF)

---

N. P. Rønneest · K. V. Gernaey (✉)  
Department of Chemical and Biochemical Engineering,  
Technical University of Denmark, Building 229,  
2800 Kgs. Lyngby, Denmark  
e-mail: kvg@kt.dtu.dk

N. P. Rønneest  
e-mail: nap@kt.dtu.dk

S. M. Stocks  
Novozymes AS, Smørmosevej 25 (2 J.S12), 2880 Bagsværd,  
Denmark

A. Eliasson Lantz  
Department of Systems Biology, Technical University  
of Denmark, Building 223, 2800 Kgs. Lyngby, Denmark

spectroscopy. This study evaluates the use of scanning and dual frequency DE spectroscopy, simple software sensors, turbidity, and MWF spectroscopy.

Online turbidity probes are commercially available at a relatively low price. Turbidity probes measure the absorbance of light in a limited range, which may be in the visible or in the NIR region. Measurements in the NIR region offer some advantages because colored compounds do not interfere in this range. In a recent comparison, Kiviharju et al. [16] concluded that a commercial turbidity probe measuring in the NIR range was superior to DE spectroscopy for the measurement of biomass in a range of bacterial and yeast cultivations. The experiments also included cultivations with the filamentous organism *Streptomyces peucetius*, but the results for the turbidity probe were not reported. The advantages of the turbidity probe include robustness, and the fact that optical density is an established offline measure of biomass concentration. The main disadvantages are its limited range of linearity, its sensitivity to interference from air bubbles and particulate matter, and its dependence on cell morphology, which is particularly problematic in processes with filamentous organisms.

Dielectric spectroscopy is based on the charge separation across the insulating cell membrane. Online DE spectroscopy has mainly been used for the monitoring of biomass concentrations in cultivations with unicellular organisms [2, 3, 6, 21, 26, 28, 36]. In filamentous systems, good correlations between biomass concentration and capacitance have been obtained online in the exponential, transition, and stationary growth phases [24, 31]. However, different correlations between biomass and capacitance were observed in the biomass decline phase [24, 31]. Recently, scanning DE spectroscopy has made it possible to obtain capacitance measurements over a range of frequencies, which may provide additional information about the size and distribution of cells. To our knowledge, this has not previously been applied to filamentous cultivations. The advantages of DE spectroscopy include a broad range of linearity, the selectivity to live biomass, and its insensitivity to other particulate matter [13]. The main disadvantages are the effects of changes in the conductivity of the medium and problems with polarization of the probe, causing noise in the measurements.

In multi-wavelength fluorescence spectroscopy, a 2D landscape covering several emission and excitation wavelengths is measured, which makes it possible to quantify a number of biological fluorophores, such as proteins and cofactors in the cultivation broth. MWF spectroscopy has been used for monitoring of biomass in a number of studies including both unicellular and filamentous organisms [5, 11, 30]. The main advantages of

MWF spectroscopy are its sensitivity and selectivity towards fluorescent compounds. Furthermore, under the right conditions, MWF spectroscopy can provide additional information about the metabolic state of the organisms [12]. The use of MWF spectroscopy for the estimation of biomass concentration depends on the correlation between the biological fluorophores and the biomass concentration, which may only be applicable under certain process conditions [8, 18, 29].

Software sensors based on classical monitoring data, such as the carbon dioxide evolution rate (CER), the oxygen uptake rate (OUR), and the base consumption, have been developed for the estimation of biomass concentrations in a number of cultivation systems [15, 29, 33]. The CER and base consumption are closely related to the growth of biomass, but the validity of the predictions is based on the assumption that the yields are constant or at least predictable. The advantages of the software sensors include their low price and the significant amount of experience and knowledge accumulated on how to analyze CER and OUR owing to their established use for monitoring in the biotechnological industry.

The development of suitable online biomass sensors has been going on for decades, but as far as we know, most of the above-mentioned sensors have only found limited application in the bioprocess industry so far. This illustrates the difficulty of measuring the biomass concentration and the high requirements of industry with respect to accuracy, robustness, and the range of applicability of the sensors. Different stages of industrial production, such as process development or large-scale production, present different requirements for the sensors. The process development, with its high level of process variation, requires robust sensors that are quickly calibrated. So far, the majority of studies concerning online biomass sensors have focused on measurements in similar processes [7, 16, 22, 24, 26, 36]. A few previous studies have included some process variation, most commonly different carbon sources and different concentration levels in the medium [3, 11, 15, 29, 33].

The aim of this study was to test and compare some of the most prominent online biomass sensors in the development of a filamentous cultivation process. Firstly, the sensors were calibrated both individually and in combination in order to compare their performance. The results are presented on the basis of all of the cultivations from the process development (eight batches). We then tested whether a selected biomass sensor could be calibrated and used for biomass estimation *during* the short process development. Furthermore, the biomass sensor was combined with a simple supervision strategy to explore whether this could improve the usability of the sensor.

## Materials and methods

### Overview of the cultivations

In total eight cultivations were run as part of a process development study aimed at improving the antibiotic titer by changing the medium, pH, and feed mode (Table 1). In batches A1–4 the batch medium and the feed were solutions of glucose, casamino acids, salts, and vitamins. In the feed, the nutrient concentrations were multiplied by a factor of 3 compared to the batch medium except for the trace metals and vitamins which were only multiplied by a factor of 2. In batches B1 and B2 the feed was a pure glucose solution. Hence, the concentrations of amino acids, salts, and vitamins added at the start of the cultivation should be enough to support both the batch and the fed-batch phases. Therefore the amounts added initially corresponded to the total amount added in A, i.e., the sum of what was added initially and what was added with the feed. In batches C1 and C2, the batch medium and the feed were the same as in batches B1 and B2, except for a doubling of the phosphate concentration and a corresponding adjustment of  $K_2SO_4$  and  $Na_2SO_4$  to keep levels of  $K^+$  and  $Na^+$  constant. Furthermore,  $SO_4^{2-}$  salts were used instead of  $Cl^-$  salts to allow in situ sterilization.

### Strain and culture conditions

*Streptomyces coelicolor* A3(2) M145 was used in all the cultivations and was a kind gift from Mervyn Bibb, John Innes Centre, Norwich, UK. The strain was preserved as a spore suspension at  $-20^\circ C$  for a maximum of 6 months. The spore suspension was made by incubating the strain on MS agar plates [14] for 10 days and harvesting the spores into 20% glycerol (w/w). The bioreactor was inoculated with 1 ml/l spore suspension ( $10^4$  spores/ml), which was thawed immediately before the inoculation. The cultivations were carried out in stainless steel bioreactors (BIO-STAT Cplus 10-3, Sartorius, Melsungen, Germany). The

initial volume was 5 l which was increased to around 9 l at the end of the fed-batch phase. The bioreactors were operated at  $30^\circ C$  and pH was controlled at either 5.9 or 6.9. The aeration rate was kept approximately constant at 1 vvm throughout the cultivations by adjusting the aeration rate in steps as the volume increased. The agitation was 600 rpm. The feed was started after a sustained drop in the CER was observed. The feed rate was adjusted to control the dissolved oxygen concentration according to a predefined profile: ramp from 80 to 20% over the first 48 h of the fed-batch phase after which the target value remained at 20%. The two different feed modes applied can be described as “pulse-pause” (constant feed rate interrupted by pauses of 6 min) or “continuous” (uninterrupted feeding where the feed rate can be changed continuously). The pulse-pause effect is a patent-protected method known to reduce the viscosity of the broth through controlled fragmentation or morphological control of the biomass (World patent WO 2003/029439) [4]. To suppress foam formation, 100  $\mu$ l/l Antifoam 206 (Sigma–Aldrich, St. Louis, MO, USA) was added at four time points during the cultivations and additionally if formation of foam was observed. The batches were stopped when the feed was depleted. Batches A2 and A4 were terminated earlier, at around 80 h, because of excessive foaming.

### Medium

The composition of the cultivation medium and feed is summarized in Table 2. The trace metal solution contained 20 mM  $FeCl_3$ , 10 mM  $CuCl_2$ , 50 mM  $ZnCl_2$ , 10 mM  $MnCl_2$ , 20  $\mu$ M  $Na_2MoO_4$ , 20 mM  $CoCl_2$ , and 10 mM  $H_3BO_4$ . The vitamin solution contained 50 mg/l biotin, 1 g/l Ca pantothenate, 1 g/l nicotinic acid, 25 g/l *myo*-inositol, 1 g/l thiamine hydrochloride, 1 g/l pyridoxine hydrochloride, and 0.2 g/l *para*-aminobenzoic acid. All medium components except glucose, chloride salts, trace elements, and vitamins were autoclaved in the bioreactor. Glucose was autoclaved separately with the chloride salts, and trace elements and vitamins were added to the autoclaved bioreactor through a sterile filter.

### Analytical methods

Dry cell weight (DCW) was determined by filtration of a known volume of cultivation broth through a preweighed, predried 0.45- $\mu$ m-pore-size filter (PESU membrane, Sartorius, Melsungen, Germany). The filter was dried for 15 min at 150 W in a microwave oven and the weight gain of the filter was determined. The measurements were made in duplicate and a standard deviation of 0.97 g/l was estimated on the basis of the pooled variances. For actinorhodin extraction, 1 ml 2 M NaOH was added to 1 ml

**Table 1** Process development for antibiotic production in *Streptomyces coelicolor*

Batch	Medium	pH	Feed mode
A1	A	5.9	Continuous
A2	A	6.9	Continuous
A3	A	5.9	Pulse-pause
A4	A	6.9	Pulse-pause
B1	B	5.9	Continuous
B2	B	6.9	Continuous
C1	C	5.9	Continuous
C2	C	6.9	Continuous

**Table 2** Overview of the cultivation medium

	A	B	C
Batch medium	10 g/l Bacto casamino acids <sup>a</sup> 15 g/l glucose 10 mM KCl 2 mM Na <sub>2</sub> SO <sub>4</sub> 4 mM NaH <sub>2</sub> PO <sub>4</sub>  2 mM citric acid 1.25 mM MgCl <sub>2</sub> 0.25 mM CaCl <sub>2</sub>  5 ml/l trace metal solution 1 ml/l vitamin solution 200 µl/l Antifoam 206 <sup>b</sup>	34 g/l Bacto casamino acids <sup>a</sup> 10 g/l glucose 13 mM K <sub>2</sub> SO <sub>4</sub> 4.5 mM Na <sub>2</sub> SO <sub>4</sub> 7 mM KH <sub>2</sub> PO <sub>4</sub> 6.5 mM Na <sub>2</sub> HPO <sub>4</sub> 7 mM citric acid 13 mM MgSO <sub>4</sub> 0.85 mM CaSO <sub>4</sub> 20 mM (NH <sub>4</sub> ) <sub>2</sub> SO <sub>4</sub> 15 ml/l trace metal solution 6 ml/l vitamin solution 200 µl/l Antifoam 206 <sup>b</sup>	34 g/l Bacto casamino acids <sup>a</sup> 10 g/l glucose 8 mM K <sub>2</sub> SO <sub>4</sub>  16 mM KH <sub>2</sub> PO <sub>4</sub> 10 mM Na <sub>2</sub> HPO <sub>4</sub> 7 mM citric acid 9 mM MgSO <sub>4</sub> 0.85 mM CaSO <sub>4</sub> 20 mM (NH <sub>4</sub> ) <sub>2</sub> SO <sub>4</sub> 15 ml/l trace metal solution 6 ml/l vitamin solution 200 µl/l Antifoam 206 <sup>b</sup>
Feed	30 g/l Bacto casamino acids <sup>a</sup> 45 g/l glucose 30 mM KCl 6 mM Na <sub>2</sub> SO <sub>4</sub> 12 mM NaH <sub>2</sub> PO <sub>4</sub> 6 mM citric acid 3.75 mM MgCl <sub>2</sub> 0.75 mM CaCl <sub>2</sub> 10 ml/l trace metal solution 2 ml/l vitamin solution 600 µl/l Antifoam 206 <sup>b</sup>	780 g/l glucose	780 g/l glucose
pH control	2 M NaOH 1 M H <sub>2</sub> SO <sub>4</sub>	2 M NH <sub>4</sub> OH 1 M H <sub>2</sub> SO <sub>4</sub>	2 M NH <sub>4</sub> OH 1 M H <sub>2</sub> SO <sub>4</sub>

<sup>a</sup> BD Biosciences, Franklin Lakes, NJ, USA

<sup>b</sup> Sigma-Aldrich, St. Louis, MO, USA

culture broth, the sample was mixed, and the biomass was separated by centrifugation of the sample at 10,000 *g* for 5 min. The actinorhodin concentration was determined by measuring the absorbance of the supernatant at 640 nm, using an extinction coefficient of 25,320 cm<sup>-1</sup> M<sup>-1</sup>. Particle size distribution was measured by the laser diffraction method on a Mastersizer 2000 with a Hydro SM manual small sample dispersion unit (Malvern Instruments Ltd., Malvern, Worcestershire, UK). The dispersions were made by adding small amounts of cultivation broth to distilled water in the dispersion unit until a laser saturation of approximately 12–15% was obtained. The refractive index of the cell pellets was set to 1.52 and the absorbance to 0.1. Mie theory was applied for deconvolution of the size distribution. Three successive measurements were made for each sample and the average was calculated. The results were verified by microscopy.

#### Online data collection

Feed rate, added acid and base (calculated on the basis of flow rates), weight of feed bottle, temperature, pH, and dissolved oxygen concentration were logged in BioPAT MFCS/win (Sartorius, Melsungen, Germany). Carbon dioxide and oxygen in the off-gas were monitored continuously with an acoustic gas analyzer (Innova 1313 Fermentation Monitor, LumaSense Technologies, Ballerup, Denmark) and logged in BioPAT MFCS/win. The classical monitoring data consisted of the following variables: time, acid added, base added, feed added, CO<sub>2</sub> concentration in exhaust, O<sub>2</sub> in exhaust, pO<sub>2</sub>, feed rate, pH, aeration rate, temperature, volume, OUR, CER, cumulative CER, cumulative OUR, sqrt(cumulative CER), sqrt(cumulative CER), derivative of CER, and cumulative DOT.

Online turbidity was measured with a Fundalux II probe (Sartorius, Melsungen, Germany) with an optical path of 10 mm and measurement range between 840 and 910 nm. The probe was introduced directly into the reactor and connected to the bioreactor control unit. Data were logged in BioPAT MFCS/win.

Fluorescence spectra were collected with a BioView spectrofluorometer (Delta, Hørsholm, Denmark), measuring through a borosilicate glass window placed in the lower part of the bioreactor. Each recorded spectrum was the average of five scans, with excitation wavelengths ranging from 270 to 550 nm in steps of 20 nm, and emission wavelengths ranging from 310 to 590 nm, also in steps of 20 nm. The data were collected in the BioView control software (Delta, Hørsholm, Denmark). The instrument has been described previously in detail by Lindemann et al. [19] and Marose et al. [23].

The dielectric spectroscopic measurements were done with the Biomass Monitor 220 (Aber Instruments, Aberystwyth, UK). The spectrometer was equipped with a 25-mm-diameter probe containing four electrodes. The probe was introduced directly into the reactor and sterilized in situ. During the cultivations, 25 frequencies from 0.1 to 20 MHz were scanned every 1 min and the capacitance as well as the conductance of the cell suspension were registered at each frequency. The data were collected and stored in AberScan (Aber Instruments, Aberystwyth, UK). Because of the significant level of noise, all data were smoothed with respect to time using an exponential moving average given by

$$S_n = (1 - \lambda)Y_n + \lambda S_{n-1}$$

where  $S_n$  and  $S_{n-1}$  are the smoothed values at time  $n$  and  $n-1$  respectively,  $Y_n$  is the measurement at time  $n$ , and  $\lambda$  is the smoothing constant.  $\lambda$  was set to 0.97 to provide the best possible smoothing while retaining the dynamics of the signal.

#### Data analysis

All data analysis was performed in MATLAB (MathWorks Inc., Natick, MA, USA) and using the PLS Toolbox for MATLAB (Eigenvector Research Inc., Wenatchee, WA, USA). Prior to the analysis, all data sets were checked for outliers by inspection of principal component analysis (PCA) scores, Hotelling's  $T^2$ , and  $Q$  residuals.

The single-variable data (turbidity, cumulative CER, and dual frequency DE spectroscopy measurements (measured at 465 kHz and 10,085 kHz)) were transformed appropriately and prediction models for the biomass concentration were estimated on the basis of a least-squares fit. The multivariable data with only two or three variables (combination of sensors) were modeled with standard multiple linear

regression models. The multivariable data with more than three variables (dielectric scans, MWF, classical monitoring data) were modeled using partial least-squares (PLS) regression with and without variable selection and various pretreatments of the data. Table 3 summarizes the tested data pretreatment and variable selection methods. For the MWF data, the use of subsets of the data for calibration and validation was also evaluated, thus decreasing the variation by only including batches with the same pH or medium (Table 3). In addition, parallel factor analysis (PARAFAC) was performed on the MWF spectra to identify the contributing fluorophores. The theoretical Cole–Cole equation was fitted to the dielectric spectral data (capacitance and conductance) by the method described in [7].

In order to compare the different model types, all model calibration and validation was performed in the same way by using a repeated calibration and validation scheme. The models were calibrated on seven batches and validated on the remaining batch. This was repeated eight times, each time leaving a new batch for validation. The root mean square error of prediction (RMSEP) was calculated for each batch and finally the mean and standard deviation of the RMSEP were calculated on the basis of the results for the eight validation batches.

## Results

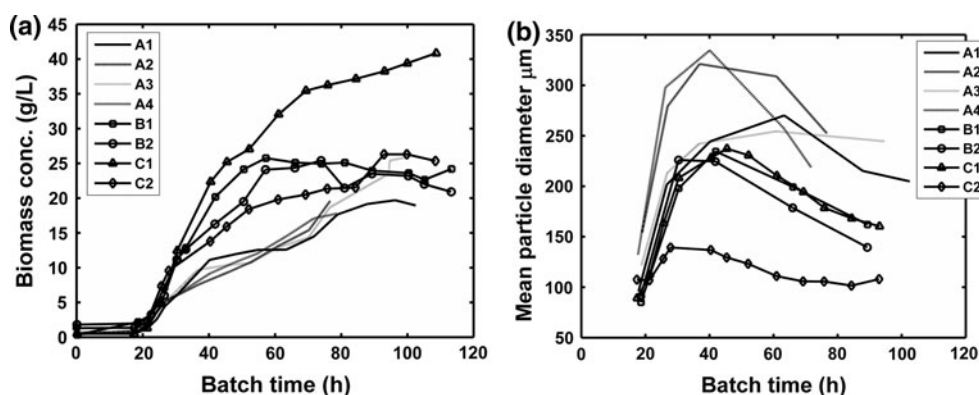
The eight batches attained final biomass concentrations ranging from 18 to 41 g/l DCW (Fig. 1a). Seven batches reached final biomass concentrations between 18 and 26 g/l DCW whereas the remaining batch (C1) reached 41 g/l DCW and can be considered as an outlier. A very large difference between morphologies of the different batches was observed as indicated by the mean particle diameter of the cell clumps (Fig. 1b). Furthermore, a change in morphology was observed during each batch. The clump diameter generally increased in the batch phase. Between 30 and 50 h a population of smaller clumps with diameter around 100–150  $\mu\text{m}$  appeared. This population continued to grow with increasing diameter and covering an increasing percentage of the total biomass volume. Because of the relative increase in the amount of smaller clumps, this appears as an overall decrease in the mean particle diameter (Fig. 1b). The final antibiotic titer varied from 225 to 6,405 mg/l as a result of the process development work. This illustrates large differences in the secondary metabolism.

#### Prediction of biomass concentration

Prediction models for the biomass concentration were calibrated on the basis of each of the online sensors as well

**Table 3** Overview of pretreatments, variable selection methods, and partitioning of the data tested for modeling of multivariable data

Data	Pretreatment	Variable selection	Partitioning of the data set
MWF spectra	No pretreatment	Whole spectrum	Partition based on pH
	Subtraction of first spectrum	Genetic algorithms	(group 1, A1, A3, B1, C1; group 2, A2, A4, B2, C2)
	Mean centering		Partition based on medium (group 1, A1–4; group 2, B1, B2, C1, C2)
	Autoscaling		
Classical monitoring data	No pretreatment	Whole data set	
	Autoscaling	Genetic algorithms	
Dielectric spectra	Subtraction of first spectrum	Whole spectrum	
	Subtraction of measurement at high frequency (10,085 kHz)	Successive removal of low frequency points	

**Fig. 1** Plot of the development of DCW (a) and mean particle diameter (b) in batches A1–4, B1, B2, C1, and C2

as combinations of the different sensors. A number of different approaches (variable selection, data pretreatment, and partitioning of the data set) were tested for each of the sensors and the best results were chosen for comparison with the other sensors (Table 4). The sensors have different requirements for the calibration data, i.e., the multivariable sensors generally require more data for calibration because more parameters have to be estimated. In order to make a fair comparison between the different sensor types, as a starting point the results are reported on the basis of the use of all available batches. In general, the prediction errors were high for batch C1 and results are also shown without this batch to facilitate comparison. The results of the individual sensors are described below.

#### Software sensors

Software sensors were calibrated on the basis of the cumulative CER alone and on the basis of PLS regression of the combined data set (described in “[Online data collection](#)”). A linear correlation was found between biomass concentration and the square root of the

cumulative CER, and a simple linear model was calibrated on the basis of these data. Variable selection using genetic algorithms was tested in combination with PLS regression of the combined data set. A small improvement was found by applying variable selection compared with PLS of the whole data set. However, compared with the simple model based on cumulative CER, no noteworthy improvements were found by including additional process data. The prediction error for the PLS model was  $2.2 \pm 0.6$  g/l compared with  $2.0 \pm 0.9$  g/l for the model based solely on cumulative CER. In fact, when excluding C1 and considering the sensors one at a time, the linear regression of the transformed cumulative CER provided the lowest average prediction error of the biomass concentration (Table 4). A closer look at the predictions showed that the cumulative CER mainly captured the overall development of the biomass concentration, whereas the dynamics of the growth phases was not so clearly discernable (data not shown). The biomass concentration was generally overestimated towards the end of the batches which may be explained by different biomass/CER yields in this phase.



**Table 4** Comparison of average prediction errors for DCW based on the online sensors

Sensor	Model	Mean RMSEP ± std (g/l)	
		All batches (range 0–41 g/l)	Without batch C1 (range 0–26 g/l)
Turbidity	2nd order polynomial	2.4 ± 1.3 <sup>a</sup>	2.3 ± 1.0 <sup>a</sup>
DE	Linear regression of dual frequency	3.2 ± 1.2	2.8 ± 0.6
DE	PLS	3.4 ± 1.4	2.9 ± 1.5
CER	Linear regression of sqrt(cumulative CER)	3.3 ± 2.4	2.0 ± 0.9
Classical monitoring data	PLS and variable selection with GA	3.4 ± 1.2	2.2 ± 0.6
MWF	PLS	5.9 ± 3.3	4.6 ± 2.4
Sqrt(cumulative CER), squared turbidity, dual frequency DE	Multiple linear regression	1.7 ± 0.6 <sup>a</sup>	1.5 ± 0.4 <sup>a</sup>
Sqrt(cumulative CER), dual frequency DE	Multiple linear regression	2.3 ± 1.6	1.6 ± 0.3

The mean and standard deviations of the RMSEP were calculated on the basis of the repeated model calibration and validation (see “Data analysis”)

<sup>a</sup> Without batch C2

### Turbidity

A non-linear correlation was found between the online turbidity measurements and the biomass concentration and a second-order polynomial was fitted to the data. The non-linearity may occur close to saturation of the sensor and/or may be influenced by changes in the size distribution of the cell pellets, which tended to first increase in the growth phase and then decrease in the production phase (Fig. 1b). Both C1 and C2 showed different correlations between the biomass concentration and the turbidity measurements. For C2 this was clearly caused by a significantly smaller pellet size in this particular batch. For C1 this was most likely caused by non-linear effects close to saturation of the sensor. When excluding batches C1 and C2, the online turbidity sensor provided prediction errors in the same order of magnitude as DE spectroscopy and the CER (2.3 ± 1.0 g/l compared with 2.8 ± 0.6 g/l and 2.0 ± 0.9 g/l for DE spectroscopy and CER, respectively.)

### Dielectric spectroscopy

The dielectric spectra were very noisy, particularly in the low frequency range, and they were therefore smoothed prior to modeling. It was chosen to use a moving average filter with exponential weights, which is also suitable for online estimation. The conductivity varied greatly between the different batches. In batches A1–4, the concentration of salts was relatively low initially but increased in the fed-batch phase because of the addition of concentrated medium with salts and acid/base for pH control resulting in an increase in conductivity from 7–9 to 16–18 mS/cm. Batches B1, B2, C1, and C2 all started with a high

concentration of salts which then decreased during the cultivation resulting in a decrease in conductivity from 24–27 to 8–10 mS/cm despite addition of acid/base for pH control. The biomass concentration was estimated on the basis of linear regression and PLS regression of the capacitance data and the fitting of the theoretical Cole–Cole equation to the capacitance and conductance data respectively. In all cases the predictions improved when the measurements at 100–155 MHz were left out (measurements were subject to noise most likely caused by polarization of the probe). The prediction errors for the linear regression and PLS regression were similar in size (2.9 ± 1.5 g/l for the PLS model compared with 2.8 ± 0.6 g/l for the linear dual frequency model) and lower than for the Cole–Cole model (data not shown). Because the linear model is simpler, the further evaluation of the DE spectroscopy sensor focuses on the linear dual frequency model. The DE spectroscopy sensor provided good predictions in the growth phase capturing the dynamic development of the biomass concentration (Fig. 2). Even in batch C1, the capacitance sensor correctly predicted the fast growth in the fed-batch phase up to 30 g/l unlike any of the other sensors. However, in most batches the predicted biomass concentration decreased in the production and death phases, although the dry cell weight was stationary or slowly increasing (Fig. 2). This contributed greatly to the overall prediction errors.

### Multi-wavelength fluorescence spectroscopy

A PARAFAC analysis revealed four major peaks (explaining 98% of the variation in the spectra) at the following excitation and emission wavelength combinations: 430/470,

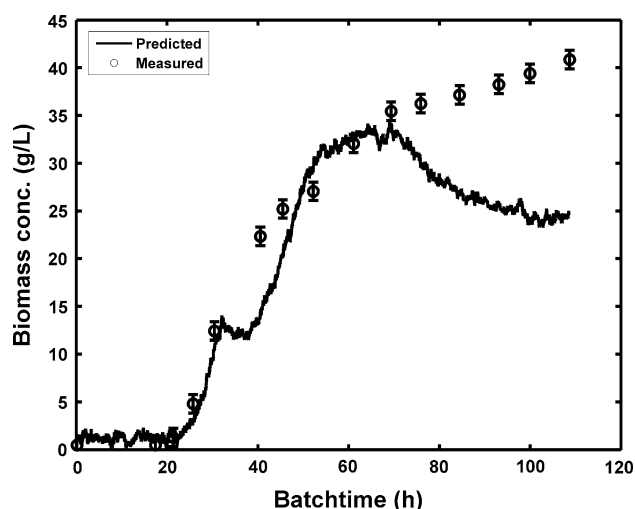


**Fig. 2** Measured and predicted DCW based on dual frequency DE spectroscopy in batch C1

380/450, 430/530, and 330/390 nm. The loading profiles of factor 2, 3, and 4 correlate well with the profiles of NAD(P)H, flavin nucleotides, and pyridoxine, respectively [10, 30] (Food Fluorescence Library, [www.models.life.ku.dk](http://www.models.life.ku.dk)). In most batches the intensity of the peaks increased from the beginning of the batch to around 30–45 h, after which the intensity decreased to a stationary level towards the end of the batch. Thus the signal was not immediately correlated to the biomass concentration. This effect may be the result of a drastic decrease in the concentration of biological fluorophores in the cell mass or/and some quenching effect or inner filter effect of the broth. It was chosen to use PLS regression of the unfolded spectra based on previous results from Ödman et al. [30]. Models were calibrated with mean centering or autoscaling (to zero mean and unit variance) of the spectra prior to the analysis. Furthermore, different partitions of the data set were tested along with variable selection using genetic algorithms (Table 3). The best results were obtained by dividing the data into two sets on the basis of the pH, autoscaling the data, and applying genetic algorithms for variable selection. However, on average for both subsets the RMSEP obtained with the MWF sensor (4.6 g/l) was higher than the RMSEPs obtained with the other sensors (2–2.9 g/l).

#### Combination of sensors

On the basis of the results we chose to test a combination of dual frequency DE spectroscopy and  $\sqrt{\text{cumulative CER}}$  as well as dual frequency DE spectroscopy,  $\sqrt{\text{cumulative CER}}$ , and the squared turbidity using multiple linear regression. Both combinations of the sensors resulted in a lowering of the prediction error and the combination of  $\sqrt{\text{cumulative CER}}$ , dual frequency DE spectroscopy,

and the squared turbidity provided the lowest prediction error of all sensors (Table 4). The prediction error was thus reduced to 1.5 g/l corresponding to 6% of the covered range of biomass concentrations. This combination was therefore chosen to test the use of an online biomass sensor and supervision strategy during process development described below.

#### Development and use of online biomass sensor during process development

The results described thus far show a comparison of the biomass sensors based on the average prediction errors for all of the available batches. In this section we explored whether the sensors can be used *during* the short process development.

The univariable sensors based on measurements of CER, dual frequency DE spectroscopy, and turbidity only require little data for calibration. It was therefore possible to calibrate a biomass sensor on the basis of these signals solely using data from batches A1 and B1. This model was subsequently used to predict the biomass concentration in the remaining batches. The predictions were computed along with a 95% confidence interval of the predictions. A simple supervision strategy was implemented on the basis of the Hotelling's  $T^2$ . The Hotelling's  $T^2$  value was calculated for each measurement point along with the 99% confidence interval on the basis of the calibration data. A Hotelling's  $T^2$  value outside the confidence limits indicated that the measurement point was different from the calibration data, and that the sensor estimations should be checked. In addition, the maximum specific growth rate was estimated on the basis of the estimated biomass concentrations.

The estimation of the multiple linear regression model resulted in an  $R^2$  of 0.98 which showed that the major part of the variation in biomass concentration in the two calibration batches was captured by the model. The biomass concentration was predicted well in batches A2, A3, and A4 (Fig. 3). In batches B2 and C2 the Hotelling's  $T^2$  values rose above the 99% confidence interval in periods of the cultivation which are indicated by the shaded area (Fig. 4 left). The calculation of the estimated biomass concentration and the Hotelling's  $T^2$  is only dependent on the latest output from the sensors. These calculations can therefore easily be performed online which provides the opportunity to adjust the predictions in real time. A closer look at the individual measurements of CER, turbidity, and DE spectroscopy revealed that the turbidity was larger compared with the measurements of the other two sensors in batches B2 and C2. By switching to the model based only on CER and DE spectroscopy measurements, it was possible to change the predictions (Fig. 4 right). In batch B2, the effect of the sensor change was small but in C2, the predictions



were improved significantly. For C1 the Hotelling’s  $T^2$  rose above the confidence interval around  $t = 50$  h (Fig. 5). A closer look at the individual measurements showed that the capacitance measurements were significantly higher than the two other measurements. However, by experience the capacitance measurements are very accurate during growth and thus we chose not to change the model. However, the high Hotelling’s  $T^2$  values serve as a warning that the predictions may not be trusted and additional offline samples can be taken to check the predictions of the model.

**Discussion**

**Multivariable sensors**

Comparison of the online sensors over a wide range of process conditions showed that the detailed information provided by the advanced sensors based on MWF and scanning DE spectroscopy did not provide better predictions of the DCW than the simpler sensors based on CER, turbidity, and dual frequency DE spectroscopy. Using MWF, Ödman et al. [30] obtained good results for the prediction of biomass concentration in *Streptomyces*

*coelicolor* cultivations over a relatively wide range of process conditions. However, under the increased process variation imposed in our experiments, a characteristic of most process development studies in laboratories or pilot plants, MWF failed to produce reliable estimations of the DCW. This may be explained by the differences in pH, which are known to have a large effect on the fluorescent properties of fluorophores [34]. Moreover, cell metabolism varied greatly in the batches as observed from the growth curves and the antibiotic production. Thus it is likely that the correlation between DCW and the biological fluorophores such as NAD(P)H and flavins was not the same in all batches. Finally, the great variation in growth and secondary metabolism may result in different levels of quenching or/and inner filter effects, making it more difficult to correct for these.

For DE spectroscopy, Dabros et al. [7] found it advantageous to use the full spectrum for prediction of biomass concentration under noisy conditions caused by interference from reactor components in small-scale reactors. We did not come to a similar conclusion, and the explanation for this may be either the substantial smoothing applied prior to modeling in our work or smaller noise levels. Overall it is likely that the more advanced sensors will perform better

**Fig. 3** Predictions of DCW based on CER, DE, and turbidity measurements in batches A2 (a), A3 (b), and A4 (c)

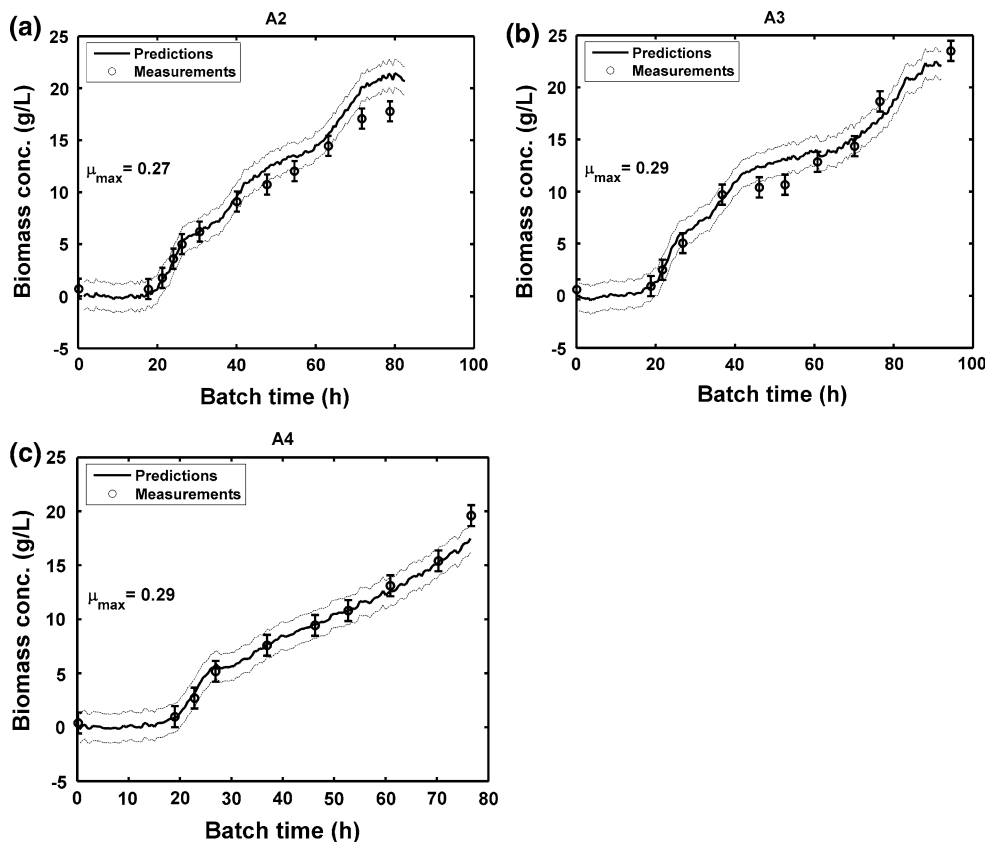


**Fig. 4** Predictions of DCW based on CER, DE, and turbidity measurements for batches B2 and C2. **a, c** Original predictions based on CER, DE spectroscopy, and turbidity measurements. The *gray shaded areas* show the time intervals in which the Hotelling's  $T^2$  values were above the 99% confidence interval, which indicate measurements that are dissimilar to the calibration data. **b, d** Predictions resulting from the switch between two different sensors: In the first part predictions are based on CER, DE spectroscopy, and turbidity and after the switch, marked by the *vertical line*, predictions are based on CER and DE spectroscopy

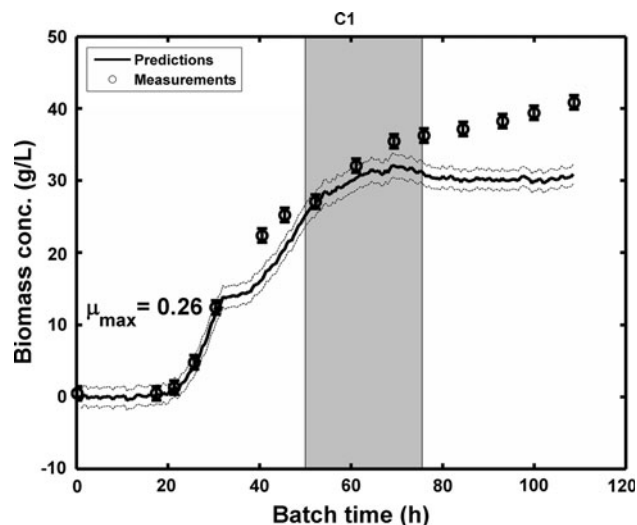
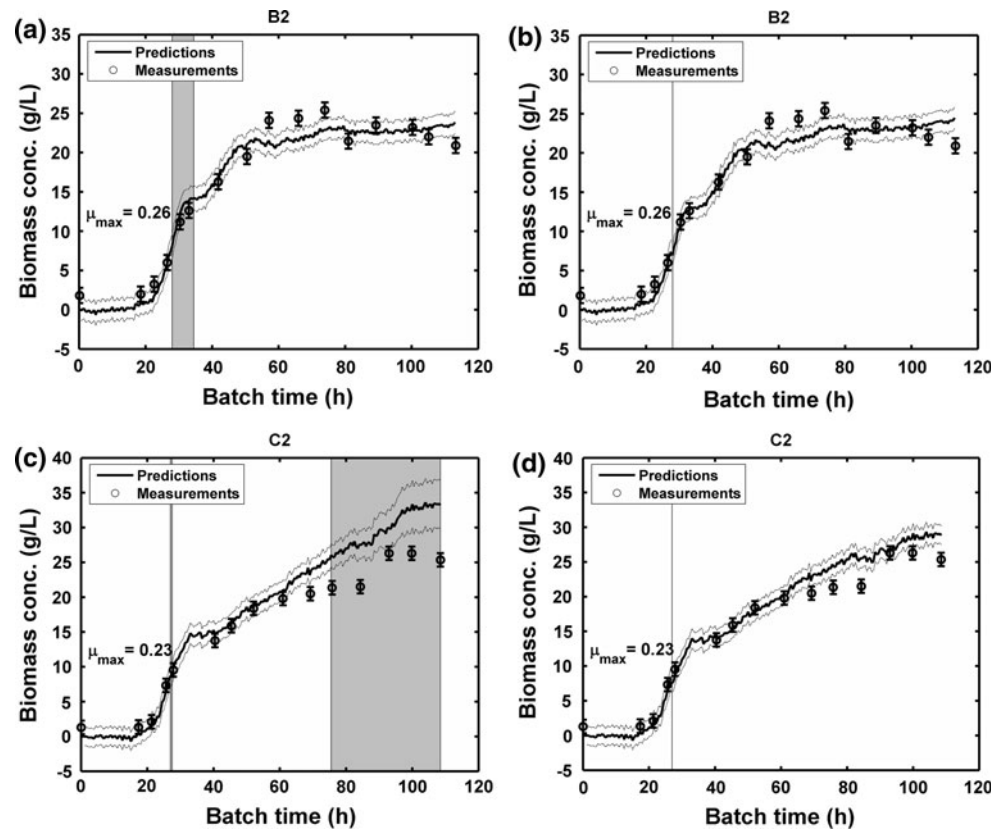


**Fig. 5** Predictions of DCW based on CER, DE spectroscopy, and turbidity measurements in batch C1. The *gray shaded areas* indicate the periods in which the Hotelling's  $T^2$  was above the 99% confidence interval

under less varying process conditions, where they have the potential to provide additional information, e.g., about cell metabolism or cell morphology [7, 12, 32]. The more advanced sensors could, for example, be implemented during the later stages of process development where only smaller changes are made to the protocol.

#### Univariable sensors

Predictions of the biomass concentration based on the online turbidity measurements are influenced by the morphology of the cells because the scattering properties are related to particle size and shape [35]. Nonetheless, the predictions of the biomass concentration were relatively accurate over a wide range of morphologies. In fact, large prediction errors mainly occurred in batch C2, in which the morphology of the cells was significantly different from the other batches (Fig. 1b).

Dual frequency DE spectroscopy provided accurate predictions of the DCW during growth, but generally gave relatively large prediction errors in the production and death phases. This is in agreement with previous observations in filamentous systems [24, 31] and in cell cultures, where the effect was partly attributed to decreases in cell viability, decreases in cell size, changes in the intracellular conductivity, and changes in the capacitance-per-unit membrane area [1, 2, 25, 28]. Alternatively, the effect might have been caused by changes in the ratio between cell mass and cell volume, because capacitance is proportional to the cell volume [13].

The prediction of biomass concentration based on the CER is an indirect method, which is based on the assumption that the biomass/carbon dioxide yield is constant. However, the predictions of biomass concentration

based on CER were robust over a relatively wide range of process variation. In fact the sensor based on CER performed as well as or better than the more direct sensors over the range covered by the batches A1–4, B1, B2, and C2.

Although the DE spectroscopy and the turbidity sensors directly measure a physical property of the biomass, the prediction of DCW is still based on correlations which are subject to changes caused by differences in morphology, cell viability, etc. It can be discussed whether the DCW is the best measure of biomass concentration because it does not differentiate between viable or dead cell mass. In some applications it may be that the information provided from the online sensors is actually a better measure of biomass, for example, dielectric measurements of viable biomass [9, 24]. However, in this study, it was important to use one established measure of biomass concentration as a reference to facilitate the comparison. When the advanced biomass sensors have won wider acceptance in industry, it is likely that the sensor measurements will be used directly as a measure of biomass concentration.

#### Combination of sensors

The CER, DE spectroscopy, and turbidity measurements can all be used individually to provide relatively accurate estimations of DCW over a wide range of process conditions. However, the predictions were improved by combining the three different sensors measuring different properties of the biomass, thus creating a positive averaging effect. Furthermore, differences between the sensor signals may provide additional information. Because the DE spectroscopy signal reflects the amount of viable biomass and the two other sensors measure total biomass, a combination of the sensors can be used to calculate the ratio between living and dead cells in real time. Similarly, a discrepancy between the predictions based on DE spectroscopy and CER on the one hand, and the turbidity probe on the other hand, suggests a different morphology, whereas differences between predictions based on CER and the other signals suggest changing yields. Finally, the use of multiple sensors makes it possible to check the individual predictions and make adjustments *online*, as was demonstrated in the last part of the results section. A combination of sensors has previously been used for the estimation of biomass concentration in cultivations. Using advanced data reconciliation, Dabros et al. [6] combined DE spectroscopy, off-gas analysis, and mid-infrared spectroscopy for the prediction of biomass and metabolite concentrations in *Saccharomyces cerevisiae* cultivations under more defined process conditions. Our results have shown that a simple combination of sensors is advantageous under more varying process conditions.

#### Application in process development

Process development represents a very important area for the application of online sensors in industry. The online sensors can provide information about the process dynamics which may be of high value in process optimization. Furthermore, the process variation will generate valuable experience and help to establish the range of validity of the sensors. However, the high level of variation requires very robust sensors. We have demonstrated that a biomass sensor based on measurements of CER, dual frequency DE spectroscopy, and turbidity can be calibrated and subsequently used to provide reliable biomass measurements *during* a short process development. Its usability was further improved by combination with estimated confidence intervals of the predictions and calculated Hotelling's  $T^2$  values, which provided information about the reliability of the predictions. This allowed the supervision of the sensor and presented the option of switching between individual sensors in real time. Biomass measurements can, for example, be used to estimate the specific growth rate online, as was also demonstrated.

#### Conclusion

The aim of this study was to compare some of the most prominent online biomass sensors during the development of a filamentous cultivation process. The results showed that the more robust univariable sensors (based on measurements of CER, turbidity, or dual frequency DE spectroscopy) provided better or no worse predictions of DCW than the more advanced multivariable sensors (based on MWF spectroscopy, scanning DE spectroscopy, multivariable modeling of classical monitoring data). Furthermore, it was shown that a combination of the sensors reduced the average and the standard deviation of the prediction errors (from  $2.0 \pm 0.9$  to  $1.5 \pm 0.4$  g/l) and provided a means of checking the sensor in real time, thus allowing operator intervention. Finally, it was shown that the biomass sensor could be calibrated and subsequently used to provide reliable biomass measurements during a short process development. This study has therefore increased our knowledge of the application of online biomass sensors under more challenging conditions, such as those observed during early process development. The process development stage represents a large potential for future applications of online sensors in industry.

**Acknowledgments** Acknowledgment is made of Insatech A/S and Aber Instruments Ltd. for the use of the Biomass Monitor 220. The Ph.D. project of Nanna Petersen Rønneest was supported by a grant from the Innovative Bioprocess Technology Research Consortium financed by the Danish Research Council for Technology and Production Sciences, Chr. Hansen A/S, Danisco A/S and Novozymes A/S.

## References

1. Ansoerge S, Esteban G, Schmid G (2007) On-line monitoring of infected Sf-9 insect cell cultures by scanning permittivity measurements and comparison with off-line biovolume measurements. *Cytotechnology* 55:115–124
2. Ansoerge S, Esteban G, Schmid G (2010) Multifrequency permittivity measurements enable on-line monitoring of changes in intracellular conductivity due to nutrient limitations during batch cultivations of CHO cells. *Biotechnol Prog* 26:272–283
3. Arnoux AS, Preziosi-Belloy L, Esteban G, Teissier P, Ghommidh C (2005) Lactic acid bacteria biomass monitoring in highly conductive media by permittivity measurements. *Biotechnol Lett* 27:1551–1557
4. Bhargava S, Wenger KS, Rane K, Rising V, Marten MR (2005) Effect of cycle time on fungal morphology, broth rheology, and recombinant enzyme productivity during pulsed addition of limiting carbon source. *Biotechnol Bioeng* 89:524–529
5. Clementschitsch F, Kern J, Pötschacher F, Bayer K (2005) Sensor combination and chemometric modelling for improved process monitoring in recombinant *E. coli* fed-batch cultivations. *J Biotechnol* 120:183–197
6. Dabros M, Amrhein M, Bonvin D, Marison IW, von Stockar U (2009) Data reconciliation of concentration estimates from mid-infrared and dielectric spectral measurements for improved on-line monitoring of bioprocesses. *Biotechnol Prog* 25:578–588
7. Dabros M, Dennewald D, Currie DJ, Lee MH, Todd RW, Marison IW, von Stockar U (2009) Cole-Cole, linear and multivariate modeling of capacitance data for on-line monitoring of biomass. *Bioprocess Biosyst Eng* 32:161–173
8. Eliasson Lantz A, Jørgensen P, Poulsen E, Lindemann C, Olsson L (2006) Determination of cell mass and polymyxin using multi-wavelength fluorescence. *J Biotechnol* 121:544–554
9. Guan Y, Evans PM, Kemp RB (1998) Specific heat flow rate: an online monitor and potential control variable of specific metabolic rate in animal cell culture that combines microcalorimetry with dielectric spectroscopy. *Biotechnol Bioeng* 58:464–477
10. Haack MB, Eliasson A, Olsson L (2004) On-line cell mass monitoring of *Saccharomyces cerevisiae* cultivations by multi-wavelength fluorescence. *J Biotechnol* 114:199–208
11. Haack MB, Eliasson Lantz A, Mortensen PP, Olsson L (2007) Chemometric analysis of in-line multi-wavelength fluorescence measurements obtained during cultivations with a lipase producing *Aspergillus oryzae* strain. *Biotechnol Bioeng* 96:904–913
12. Hantelmann K, Kollmeier M, Hüll D, Hitzmann B, Scheper T (2006) Two-dimensional fluorescence spectroscopy: a novel approach for controlling fed-batch cultivations. *J Biotechnol* 121:410–417
13. Harris CM, Todd RW, Bungard SJ, Lovitt RW, Morris JG, Kell DB (1987) Dielectric permittivity of microbial suspensions at radio frequencies: a novel method for the real-time estimation of microbial biomass. *Enzyme Microb Technol* 9:181–186
14. Hobbs G, Frazer CM, Gardner DC, Cullum JA, Oliver SG (1989) Dispersed growth of *Streptomyces* in liquid culture. *Appl Microbiol Biotechnol* 31:272–277
15. Jenzsch M, Simutis R, Eisbrenner G, Stückrath I, Lübbert A (2006) Estimation of biomass concentrations in fermentation processes for recombinant protein production. *Bioprocess Biosyst Eng* 29:19–27
16. Kiviharju K, Salonen K, Moilanen U, Meskanen E, Leisola M, Eerikäinen T (2007) On-line biomass measurements in bioreactor cultivations: comparison study of two on-line probes. *J Ind Microbiol Biotechnol* 34:561–566
17. Kiviharju K, Salonen K, Moilanen U, Eerikäinen T (2008) Biomass measurement online: the performance of in situ measurements and software sensors. *J Ind Microbiol Biotechnol* 35:657–665
18. Li JK, Asali EC, Humphrey AE, Horvath JJ (1991) Monitoring cell concentration and activity by multiple excitation fluorometry. *Biotechnol Prog* 7:21–27
19. Lindemann C, Marose S, Nielsen HO, Scheper T (1998) 2-Dimensional fluorescence spectroscopy for on-line bioprocess monitoring. *Sens Actuators B Chem* 51:273–277
20. Madrid RE, Felice CJ (2005) Microbial biomass estimation. *Crit Rev Biotechnol* 25:97–112
21. Markx GH, Davey CL, Kell DB (1991) The permittostat a novel type of turbidostat. *J Gen Microbiol* 137:737–744
22. Markx GH, Davey CL, Kell DB, Morris P (1991) The dielectric permittivity at radio frequencies and the Bruggeman probe: novel techniques for the on-line determination of biomass concentrations in plant cell cultures. *J Biotechnol* 20:279–290
23. Marose S, Lindemann C, Scheper T (1998) Two-dimensional fluorescence spectroscopy: a new tool for on-line bioprocess monitoring. *Biotechnol Prog* 14:63–74
24. Neves AA, Pereira DA, Vieira LM, Menezes JC (2000) Real time monitoring biomass concentration in *Streptomyces clavuligerus* cultivations with industrial media using a capacitance probe. *J Biotechnol* 84:45–52
25. Noll T, Biselli M (1998) Dielectric spectroscopy in the cultivation of suspended and immobilized hybridoma cells. *J Biotechnol* 63:187–198
26. November EJ, Van Impe JF (2000) Evaluation of on-line viable biomass measurements during fermentations of *Candida utilis*. *Bioprocess Eng* 23:473–477
27. Olsson L, Nielsen J (1997) Online and in situ monitoring of biomass in submerged cultivations. *Trends Biotechnol* 15:517–522
28. Opel CF, Li J, Amanullah A (2010) Quantitative modeling of viable cell density, cell size, intracellular conductivity, and membrane capacitance in batch and fed-batch CHO processes using dielectric spectroscopy. *Biotechnol Prog* 26:1187–1199
29. Ödman P, Johansen CL, Olsson L, Gernaey KV, Eliasson Lantz A (2009) On-line estimation of biomass, glucose and ethanol in *Saccharomyces cerevisiae* cultivations using in situ multi-wavelength fluorescence and software sensors. *J Biotechnol* 144:102–112
30. Ödman P, Johansen C, Olsson L, Gernaey KV, Eliasson Lantz A (2010) Sensor combination and chemometric variable selection for online monitoring of *Streptomyces coelicolor* fed-batch cultivations. *Appl Microbiol Biotechnol* 86:1745–1759
31. Sarra M, Ison AP, Lilly MD (1996) The relationships between biomass concentration, determined by a capacitance-based probe, rheology and morphology of *Saccharopolyspora erythraea* cultures. *J Biotechnol* 51:157–165
32. Siano SA (1997) Biomass measurement by inductive permittivity. *Biotechnol Bioeng* 55:289–304
33. Sundström H, Enfors S (2008) Software sensors for fermentation processes. *Bioprocess Biosyst Eng* 31:145–152
34. Valeur B (2001) Molecular fluorescence: principles and applications. Wiley-VCH, Weinheim, Germany
35. Williams P, Norris K (1987) Near-infrared technology in the agricultural and food industries. American Association of Cereal Chemists, Minnesota, USA
36. Xiong Z, Guo M, Guo Y, Chu J, Zhuang Y, Zhang S (2008) Real-time viable-cell mass monitoring in high-cell-density fed-batch glutathione fermentation by *Saccharomyces cerevisiae* T65 in industrial complex medium. *J Biosci Bioeng* 105:409–413